ISSN 1070-3284, Russian Journal of Coordination Chemistry, 2024, Vol. 50, No. 7, pp. 512–522. © Pleiades Publishing, Ltd., 2024.

Pseudopolymeric Thallium(I) Di-*iso*-pentyl Dithiophosphate, [Tl{$S_2P(O\text{-}iso\text{-}C_5H_{11})_2$}]: Synthesis, Structural Organization (Role of Secondary Tl···S and Tl···O Interactions in Supramolecular Self-Assembly), and Thermal Behavior

O. A. Bredyuk[a], I. A. Lutsenko[b], Yu. V. Nelyubina[c], S. V. Zinchenko[d], and A. V. Ivanov[a, *]

[a] *Institute of Geology and Nature Management, Far Eastern Branch, Russian Academy of Sciences, Blagoveschensk, Russia*

[b] *Kurnakov Institute of General and Inorganic Chemistry, Russian Academy of Sciences, Moscow, Russia*

[c] *Nesmeyanov Institute of Organoelement Compounds, Russian Academy of Sciences, Moscow, Russia*

[d] *Favorsky Institute of Chemistry, Siberian Branch, Russian Academy of Sciences, Irkutsk, Russia*

**e-mail: alexander.v.ivanov@chemist.com*

Received March 12, 2024; revised April 3, 2024; accepted April 3, 2024

Abstract—Crystalline pseudopolymeric thallium(I) di-*iso*-pentyl dithiophosphate (Dtph), [Tl{$S_2P(O\text{-}iso\text{-}C_5H_{11})_2$}] (**I**), is synthesized and characterized in detail by single-crystal XRD (CIF file CCDC no. 2296421), simultaneous thermal analysis (STA), multinuclear (^1H, ^{13}C, ^{31}P) NMR, and IR spectroscopy. Nonequivalent molecules of two types containing Tl(1) and Tl(2) atoms (hereinafter molecules *A* and *B* , respectively) are involved (1 : 1) in the formation of the structure of compound **I**. In both molecules, the *S*,*S*'-anisobidentate coordination of the Dtph ligands (Tl–S bond lengths 3.006–3.092 Å) results in the formation of small-size four-membered metallocycles [TlS_2P] (a 'butterfly' conformation) with significantly averaged P–S bond lengths (1.966–1.985 Å). Molecules *A* and *B* are structurally ordered upon the construction of supramolecular chains of two types $(\cdots A\cdots A\cdots A\cdots)_n$ and $(\cdots B\cdots B\cdots B\cdots)_n$ with oppositely directed structural units combined by paired secondary Tl···S and Tl···O interactions alternating over the chain length. In turn, paired secondary (but weaker) Tl···S interactions occur between molecules *A* and *B* belonging to two neighboring pseudopolymeric chains. The multiplicity of these interactions provides the formation of double supramolecular ribbons. The thermal behavior of compound **I** is studied by the STA technique under an argon atmosphere. Thallium(I) tetrathiophosphate Tl_3PS_4 is identified as the only end product of the thermolysis of compound **I**. Electron probe microanalysis (EPMA) and scanning electron microscopy (SEM) are used to study the residual substance.

Keywords: thallium(I) di-*iso*-pentyl dithiophosphate, crystal structure, supramolecular self-assembly, secondary interactions (Tl···S, Tl···O), thermal behavior

DOI: 10.1134/S1070328424600529

INTRODUCTION

All thallium compounds are characterized by high toxicity [1]. However, selective anticancer activity was found for a number of the thallium(III) complexes with the dicarboxylic acid derivatives [2]. Owing to a high sulfur affinity, thallium exhibits a tendency to the formation of stable compounds with dithio reagents, in particular, with dithiocarbamate and dithiophosphate ligands. Both thallium(I) and thallium(III) dithiocarbamates are studied to a high extent and exhibit the properties of promising precursors for various microcrystalline and film thallium sulfides prepared in one-stage thermal processes, e.g., [3–5]. However, unlike the dithiocarbamates, thallium(I) dithiophosphate complexes were studied to a considerably less extent: a structural information available from scientific periodicals is restricted by a few publications only [6–10].

Continuing these studies, we isolated in preparative yields and characterized in detail (by XRD, IR and ^1H, $^{13}C\{^1H\}$, and $^{31}P\{^1H\}$ NMR spectroscopy) a new crystalline pseudopolymeric complex *catena*-poly[(*O*,*O*'-di-*iso*-pentyldithiophosphato-*S*,*S*,*S*',*S*')thallium(I)], [Tl{$S_2P(O\text{-}iso\text{-}C_5H_{11})_2$}] (**I**). It was shown for the structure of compound **I** that nonequivalent molecules of the complex (*A* for Tl(1) and *B* for Tl(2)) formed pseudopolymeric chains of two types due to the secondary Tl···S and Tl···O interactions. The pairwise combination of these chains results in the formation of supramolecular ribbons. The thermal behavior of the synthesized compound was studied by the .STA technique.

EXPERIMENTAL

Synthesis of [Tl{$S_2P(O\text{-}iso\text{-}C_5H_{11})_2$}] (I). A solution of K{$S_2P(O\text{-}iso\text{-}C_5H_{11})_2$} (**Ia**) (CHEMINOVA AGRO A/S) (0.342 g, 1.109 mmol) in water (20 mL) was poured with stirring to a solution containing $TlNO_3$ (Merck) (0.281 g, 1.055 mmol) in water (10 mL) at room temperature. A white finely crystalline precipitate that matured for a day was filtered off and dried in air. The yield was 97%. The crystals of compound **I** suitable for XRD (colorless transparent needles, m.p. = 73–74°C) were prepared from an acetone–ethanol (1 : 1) solution.

IR of compound **I** (ν, cm^{-1}): 2952, 2900, 2870 ν(C–H), 954 ν[(P)–O–C], 780 ν[P–O–(C)], 665 $\nu_{as}(PS_2)$, 571 $\nu_s(PS_2)$.

^1H NMR of **I** ($CDCl_3$; δ, ppm): 4.08 t (d, $^3J_{H-P}$ = 8.8 Hz; 4H, $OCH_2CH_2CH(CH_3)_2$); 1.83–1.69 m (2H, $OCH_2CH_2CH(CH_3)_2$); 1.62–1.57 q (4H, $OCH_2CH_2CH(CH_3)_2$); 0.93 d (12H, $OCH_2CH_2CH(CH_3)_2$). $^{13}C\{^1H\}$ NMR ($CDCl_3$; δ, ppm): 65.28 (d, $^2J_{C-P}$ = 8.2 Hz, $-OCH_2-$); 38.99 (d, $^3J_{C-P}$ = 8.4 Hz, $-CH_2-$); 24.96 (–CH<); 22.64 ($-CH_3$). ^{31}P NMR ($CDCl_3$; δ): 97.89 ppm.

For $C_{10}H_{22}O_2S_2PTl$ (**I**)

Anal. calcd., %	C, 25.35	H, 4.68	S, 13.54
Found, %	C, 25.43	H, 4.73	S, 12.91

The original potassium dithiophosphate K{$S_2P(O\text{-}iso\text{-}C_5H_{11})_2$} (**Ia**) used in the synthesis was also comparatively characterized on the IR and (^1H, $^{13}C\{^1H\}$, ^{31}P) NMR spectral data.

IR of compound **Ia** (ν, cm^{-1}): 2955, 2905, 2874 ν(C–H), 973 ν[(P)–O–C], 780 ν[P–O–(C)], 693 ν(P=S), 583 ν(P–S).

^1H NMR of **Ia** ($CDCl_3$; δ, ppm): 4.00 t (d, $^3J_{H-P}$ = 8.4 Hz; 4H, $OCH_2CH_2CH(CH_3)_2$); 1.76–1.63 m (2H, $OCH_2CH_2CH(CH_3)_2$); 1.61–1.56 q (4H, $OCH_2CH_2CH(CH_3)_2$); 0.93 d (12H, $OCH_2CH_2CH(CH_3)_2$). $^{13}C\{^1H\}$ NMR ($CDCl_3$; δ, ppm): 65.73 (d, $^2J_{C-P}$ = 7.8 Hz, $-OCH_2-$); 39.30 (d, $^3J_{C-P}$ = 8.0 Hz, $-CH_2-$); 25.18 (–CH<), 22.79 ($-CH_3$). ^{31}P NMR ($CDCl_3$; δ): 110.98 ppm.

IR spectra were recorded for the crystals of studied compounds **I** and **Ia** on a PerkinElmer Spectrum 65 FT-IR spectrometer by the attenuated total internal reflectance (ATR) method in a frequency range of 400–4000 cm^{-1}. Elemental analysis was carried out on a Carlo Erba EA 1108 automated analyzer.

The $^1H/^{13}C\{^1H\}/^{31}P\{^1H\}$ NMR spectra of complex **I** and initial salt **Ia** in a solution of 99.8% $CDCl_3$ (reagent grade, Solvex) were recorded on a BRUKER Avance 400 spectrometer with working frequencies of 400.13/100.62/161.98 MHz, a superconducting magnet (B_0 = 9.4 T), and the pulsed Fourier transform mode. The ^1H and $^{13}C/^{31}P$ isotropic chemical shifts (δ, ppm) are given relative to TMS/85% H_3PO_4.

XRD analysis of single crystals of compound **I** was conducted on a Bruker Quest D8 CMOS diffractometer (MoK_α radiation, graphite monochromator, ω scan mode) at 100 K. The structure was solved using the SHELXT program [11, 12] and refined by full-matrix least squares using the OLEX2 program [13] in the anisotropic approximation for F^2_{hkl}. In the structure of compound **I**, a significant number of atoms is statistically distributed between two structural positions. For instance, the Tl(1)/Tl(1)', S(1)/S(1)', S(2)/S(2)', O(1)/O(1)', O(2)/O(2)', and C(6)/C(6')–C(9)/C(9)' atoms are characterized by the same populations of the positions (0.5), whereas the populations are 0.706(9) and 0.294(9) for the carbon atoms C(17)–C(20) and C(17)'–C(20)', respectively. The positions of hydrogen atoms were calculated geometrically and refined in the isotropic approximation by the riding model.

The main crystallographic data and refinement parameters for the structure of compound **I** are given in Table 1. Selected bond lengths and angles are listed in Table 2.

The coordinates of atoms, bond lengths, and bond angles in the structure of compound **I** were deposited with the Cambridge Crystallographic Data Centre (CIF file CCDC no. 2296421; deposit@ccdc.cam.ac.uk or http://www.ccdc.cam.ac.uk).

The thermal behavior of compound **I** was studied by the STA method including the simultaneous detection of thermogravimetry (TG) and differential scanning calorimetry (DSC) curves. The study was conducted on an STA 449C Jupiter instrument (NETZSCH) in corundum crucibles under caps with holes providing a vapor pressure of 1 atm for the thermal decomposition of the sample. The heating rate was 5°C/min to 700°C in an argon atmosphere. The weight of the studied samples was 4.832–11.352 mg. The measurement accuracies of temperature and weight change were ±0.9°C and $\pm 1 \times 10^{-4}$ mg, respectively. When detecting TG and DSC curves, the correction file and temperature and sensitivity calibrations for the specified temperature program and heating rate were used. The independent determination of the melting point of compound **I** was carried out on a PTP(M) instrument (OAO Khimlaborpribor, Russia).

The size and morphological features of particles of the end substance formed due to the thermolysis of complex **I** were studied on a SIGMA scanning electron microscope (Zeiss) and an Aztec X-Max 80 analytical module for EPMA with the energy dispersion (resolution 124 eV). SEM images were detected at a voltage of 20 keV in the backscattered electron imaging (BEI) mode. The samples were placed on a conduc-

Table 1. Crystallographic data and experimental and structure refinement parameters for compound Tl{S_2P(O-*iso*-$C_5H_{11})_2$} (**I**)

Parameter	Value
Empirical formula	$C_{10}H_{22}O_2S_2PTl$
FW	473.73
T, K	100
Crystal system	Monoclinic
Space group	$P2_1/c$
Z	8
a, Å	16.4794(4)
b, Å	26.0884(6)
c, Å	7.36360(10)
α, deg	90
β, deg	91.7150(10)
γ, deg	90
V, Å^3	3164.35(11)
ρ_{calc}, g/cm^3	1.989
μ, cm^{-1}	105.6
F(000)	1808
Crystal size, mm	0.22 × 0.08 × 0.07
Data collection range for θ, deg	1.991–25.997
Ranges of reflection indices *hlk*	$-16 \le h \le 20$, $-32 \le k \le 32$, $-9 \le l \le 9$
Measured reflections	29576
Independent reflections (R_{int})	6193 (0.0457)
Reflections with $I > 2\sigma(I)$	5236
Refinement variables	343
GOOF	1.067
R_1, wR_2 (for $F^2 > 2\sigma(F^2)$)	0.0358, 0.0839
R_1, wR_2 (for all reflections)	0.0459, 0.0886
Residual electron density (min/max), e/Å^3	−1.125/1.881

tive coating of specialized tables, followed by deposition of a carbon layer using the method of vacuum thermal spraying on a VUP-5 setup.

RESULTS AND DISCUSSION

In the IR spectra of complex **I** and initial salt **Ia**, the bands in a range of 2955–2870 cm^{-1} are caused by stretching vibrations of the C–H bonds in the alkyl substituents of the Dtph ligand [14]. The high-intensity absorption bands at 954 and 973 cm^{-1} are assigned to stretching vibrations of the (P)–O–C bonds in compounds **I** and **Ia** [15, 16]. The medium-intensity ν[P–O–(C)] band appears in the spectra of both discussed compounds at 780 cm^{-1} [17], whereas the narrow intense peak at 693 cm^{-1} associated with vibrations of the P=S bond of the thiophosphoryl group and the medium-intensity ν(P–S) band at 583 cm^{-1} are observed only in the IR spectrum of the potassium salt indicating the predominantly ionic character of compound **Ia** [15, 17, 18]. On the contrary, the spectrum of complex **I** contains only the ν_{as}(P–S)/ν_s(P–S) vibrations at 665/571 cm^{-1} [9, 10, 15, 18], which can be explained by averaging the P–S bond lengths in the Dtph ligand upon binding to thallium(I).

The ^{1}H, ^{13}C{^{1}H}, and ^{13}P{^{1}H} NMR spectra of complex **I** (Figs. S1–S3) in a $CDCl_3$ solution (see Supplementary Information; the corresponding NMR spectra of initial salt **Ia** are presented in Figs. S4–S6) directly confirm the individual character of the studied compound and the absence of impurities. The chemical groups of alkyl substituents of the di-*iso*-pentyl dithiophosphate ligand (–OCH_2–, –CH_2–, –CH<, –CH_3) in the ^{1}H and ^{13}C{^{1}H} NMR

Table 2. Selected bond lengths (*d*) and bond (ω) and torsion (φ) angles in the structure of compound **I***

Bond	*d*, Å	Bond	*d*, Å
	Molecule *A*		
Tl(1)–S(1)'	3.089(4)	Tl(1)'–S(1)	3.074(4)
Tl(1)–S(2)'	3.062(4)	Tl(1)'–S(2)	3.092(4)
Tl(1)···S(1)[b]	3.317(5)	Tl(1)'[b]···S(2)'	3.189(4)
Tl(1)···S(2)[a]	3.409(4)	Tl(1)'[a]···S(1)'	3.408(5)
Tl(1)···O(1)[a]	3.04(2)	Tl(1)'[b]···O(1)'	3.04(2)
S(1)'–P(1)'	1.976(6)	S(1)–P(1)	1.985(6)
S(2)'–P(1)'	1.984(6)	S(2)–P(1)	1.970(6)
P(1)'–O(1)'	1.588(2)	P(1)–O(1)	1.59(2)
P(1)'–O(2)'	1.631(12)	P(1)–O(2)	1.61(1)
O(1)'–C(1)	1.53(2)	O(1)–C(1)	1.43(3)
O(2)'–C(6)'	1.45(2)	O(2)–C(6)	1.43(2)
	Molecule *B*		
Tl(2)–S(3)	3.063(2)	S(3)–P(2)	1.978(2)
Tl(2)–S(4)	3.006(2)	S(4)–P(2)	1.966(2)
Tl(2)···S(3)[a]	3.2410(15)	P(2)–O(3)	1.607(4)
Tl(2)···S(4)[b]	3.2996(15)	P(2)–O(4)	1.595(5)
Tl(2)···O(3)[a]	3.259(5)	O(3)–C(11)	1.458(8)
Tl(2)···O(4)[b]	3.290(4)	O(4)–C(16)	1.443(8)
Angle	ω, deg	Angle	ω, deg
	Molecule *A*		
S(2)'Tl(1)S(1)'	66.13(11)	S(1)Tl(1)'S(2)	65.64(10)
P(1)'S(1)'Tl(1)	85.9(2)	P(1)S(1)Tl(1)'	84.1(2)
P(1)'S(2)'Tl(1)	86.5(2)	P(1)S(2)Tl(1)'	83.9(2)
S(1)'P(1)'S(2)'	115.9(3)	S(2)P(1)S(1)	115.4(3)
O(1)'P(1)'S(1)'	112.1(9)	O(1)P(1)S(1)	112.4(9)
O(1)'P(1)'S(2)'	105.8(9)	O(1)P(1)S(2)	106.0(9)
O(2)'P(1)'S(1)'	111.5(5)	O(2)P(1)S(1)	110.6(5)
O(2)'P(1)'S(2)'	110.1(5)	O(2)P(1)S(2)	113.1(5)
O(1)'P(1)'O(2)'	100.2(6)	O(1)P(1)O(2)	98.0(6)
C(1)O(1)'P(1)'	121.8(16)	C(1)O(1)P(1)	121.8(17)
C(6)'O(2)'P(1)'	119.8(9)	C(6)O(2)P(1)	123.9(9)
	Molecule *B*		
S(4)Tl(2)S(3)	67.79(4)	O(4)P(2)S(3)	111.3(2)
P(2)S(3)Tl(2)	85.20(7)	O(4)P(2)S(4)	104.8(2)
P(2)S(4)Tl(2)	86.99(7)	O(4)P(2)O(3)	104.2(2)
S(4)P(2)S(3)	118.22(11)	C(11)O(3)P(2)	118.4(4)
O(3)P(2)S(3)	105.1(2)	C(16)O(4)P(2)	122.6(5)
O(3)P(2)S(4)	112.4(2)		
Angle	φ, deg	Angle	φ, deg
	Molecule *A*		
Tl(1)S(2)'S(1)'P(1)'	152.9(3)	Tl(1)'S(2)S(1)P(1)	141.8(3)
S(2)'Tl(1)P(1)'S(1)'	156.5(3)	S(2)Tl(1)'P(1)S(1)	147.6(3)
	Molecule *B*		
Tl(2)S(4)S(3)P(2)	164.4(1)	S(4)Tl(2)P(2)S(3)	166.8(1)

* Symmetry transforms: [a] $x, 3/2 - y, 1/2 + z$; [b] $x, 3/2 - y, -1/2 + z$.

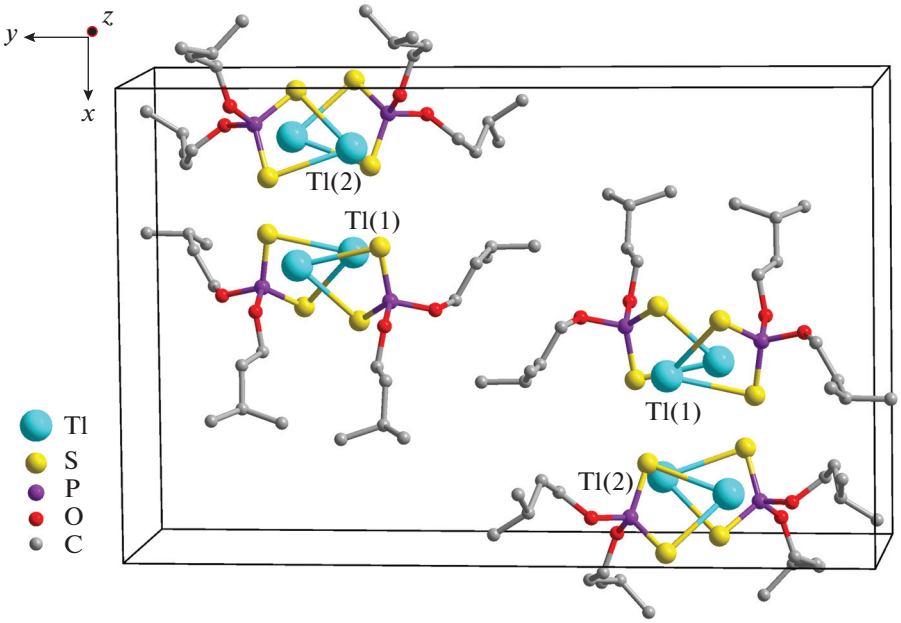

Fig. 1. Packing of molecular structural units in the crystal of compound **I**.

spectra are presented by the expected groups of resonance signals. The proton signals are presented by the corresponding multiplicity; an additional splitting of triplets (1 : 2 : 1) of the $-OCH_2-$ groups is caused by the additional spin–spin coupling (SSC) of these protons with the ^{31}P nucleus (I = 1/2): the three-bond SSC constants are $^3J_{H-P}$ = 8.8/8.4 Hz (**I**/**Ia**). For the same reason, the $-OCH_2-$ and $-CH_2-$ groups in the $^{13}C\{^1H\}$ NMR spectra of compounds **I** and **Ia** exhibit the doublet (1 : 1) signals: $^2J_{C-P}$ = 8.2/7.8 Hz and $^3J_{C-P}$ = 8.4/8.0 Hz. The value $\delta(^{31}P)$ = 97.89 ppm for compound **I** is consistent with the corresponding data for thallium(I) diethyl and di-*iso*-propyl dithiophosphates [18]. A comparative analysis of the ^{31}P and ^{13}C chemical shifts of the respective chemical groups in the studied compounds (**I** and **Ia**) shows systematically lower values for the thallium complex. Therefore, it can be concluded that the binding of the di-*iso*-pentyl dithiophosphate ligand to the metal atom results in the shift of the electron density of the latter to the Dtph ligand, toward the $[S_2PO_2]$ group of five highly electronegative sulfur, phosphorus, and oxygen atoms. A consequence of this electron density redistribution is an increase in the shielding of the ^{31}P nucleus appeared as a decrease in the $\delta(^{31}P)$-value, which was previously observed for dialkyl dithiophosphate complexes of such metals as gold(I) [19], platinum(II) [20], lead(II) [21], cadmium [22], and nickel [23]. For this reason, the efficiency of electron density shifting from the carbon atoms of the alkyl substituents toward the oxygen atom decreases in the thallium(I) complex, which is accompanied by a systematic decrease in the ^{13}C chemical shift values (compared to initial salt **Ia**).

The unit cell of complex **I** contains eight formula units $[Tl\{S_2P(O\text{-}iso\text{-}C_5H_{11})_2\}]$ (Table 1, Fig. 1). The molecules containing the Tl(1) and Tl(2) atoms are structurally nonequivalent (hereinafter molecules *A* and *B*, respectively). In molecule *A*, the majority of atoms, except for C(1)–C(5) and C(10), are disordered over two structural positions with equal populations (Figs. 2a, 2b). In molecule *B*, the structural disordering effect appears only for some carbon atoms, C(17)–C(20), in one of the chains of alkyl substituents (Fig. 2c). In the discussed molecules, the Dtph ligands exhibit an *S*,*S*′-anisobidentate mode of coordination to the central thallium atoms (the Tl–S bond lengths lie in a range of 3.006(2)–3.092(4) Å) with the formation of four-membered metallocycles $[TlS_2P]$; although the difference in the Tl–S bond lengths inside each cycle is rather low (0.018–0.057 Å). It is noteworthy that the values presented for the Tl–S bonds are intermediate between the length of the ideal covalent bond (as a sum of covalent radii of the thallium and sulfur atoms of 2.45 Å) and secondary bond[1] (as a sum of their van der Waals radii of 3.76 Å [25, 26][2]), which possibly reflects a lowered contribution of the covalent component to these bonds.

The small sizes of the $[TlS_2P]$ metallocycles are predetermined by distances between the oppositely

[1] The concept of secondary bonds was proposed [24] for the description of interactions between atoms at distances close to the sums of their van der Waals radii.

[2] It should be kept in mind that an objective demand in correcting the van der Waals radius of the thallium atom from 1.96 Å [25] toward higher values was substantiated in several works (2.47 Å [27], 2.27 Å [28], 2.59 Å [29]).

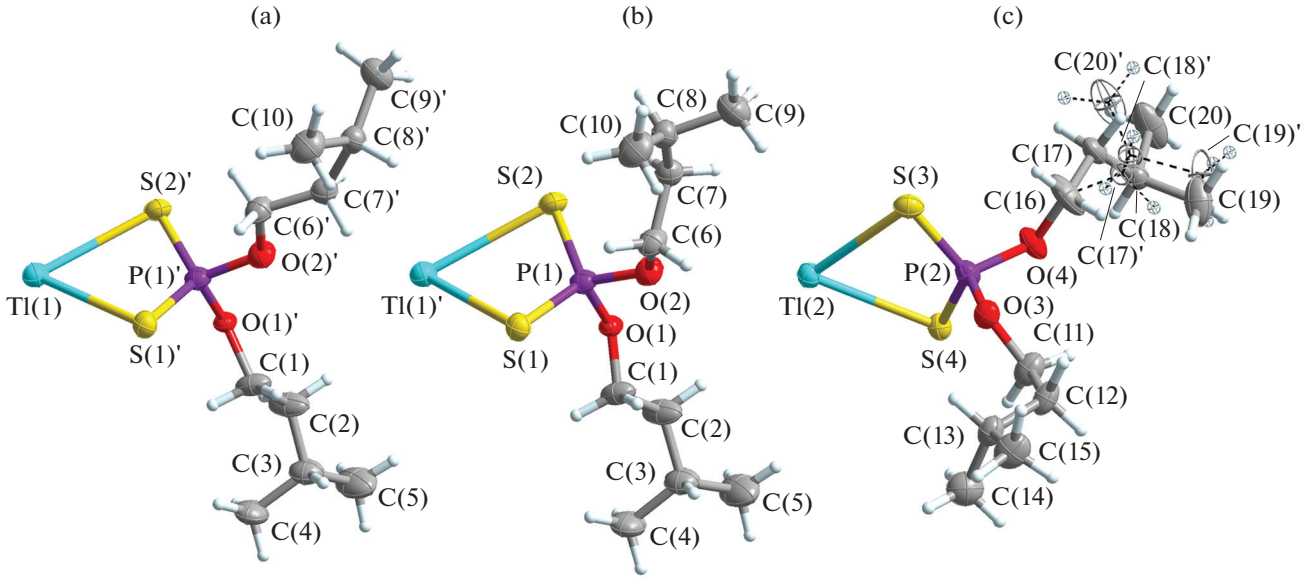

Fig. 2. Nonequivalent molecules of complex **I**: (a, b) *A* with the Tl(1) and Tl(1)' atoms and (c) *B*. Ellipsoids of 50% probability.

lying atoms: Tl···P (3.485(5)–3.545(5) Å) and S···S (3.342(6)–3.385(2) Å). In turn, the TlSSP and STlPS torsion angles that substantially deviate from 180° (see Table 2) indicate the noncoplanar configuration of the atoms in the discussed cycles. The angles between the planes of the [TlSS] and [SSP] half-cycles are the smallest ones and, hence, the geometry of the [TlS_2P] metallocycles should be approximated by a 'butterfly' conformation (with the inflection of the cycle along the S···S axis).

The phosphorus atom exists in the distorted tetrahedral environment [S_2O_2] in each of the nonequivalent Dtph ligands. As expected from the IR spectroscopy data, the P–S bond lengths lie in a narrow range of 1.966(2)–1.985(6) Å, which indicates their effective averaging due to Dtph ligand binding with thallium owing to a high π-electron density delocalization inside the formed small-size [TlS_2P] metallocycles. The C–C bond lengths in the alkyl substituents of the Dtph ligands in molecules *A*/*B* are as follows: 1.33(3), 1.48(3), 1.496(18)–1.576(18), and 1.68(3)/1.455(12)–1.570(16) Å (excluding the minor disordering component).

The subsequent structural ordering of the nonequivalent molecules (*A* and *B*) in complex **I** involves the intermolecular paired secondary interactions Tl···S and Tl···O. The discussed molecules of each type construct pseudopolymeric chains in which molecules *A* (with the Tl(1) and Tl(1)' atoms) or *B*, characterized by opposite spatial orientations, alternate along their length (Fig. 3). Since the principles of structural organization of the chains are nearly the same in both cases, we will consider their formation in more detail using as an example molecule *B* in which disordering is observed only in the peripheral part of one of the alkyl substituents. Having the single Dtph ligand and being coordinatively unsaturated, each Tl(2) thallium atom forms nonequivalent secondary Tl···S bonds with two nearest neighbors: Tl(2)···S(3)^a/S(4)^b 3.2410/3.2996 Å (Table 2, Fig. 3b). Both presented values appreciably exceed the Tl–S bond length in the metallocycles but are substantially lower than the sum of the van der Waals radii of this pair of atoms: 3.76 Å [25, 26]. The S(3)/S(4) atoms participate in the same interactions with the thallium atoms Tl(2)^b/Tl(2)^a of neighboring molecules *B*, which results in their symmetric mutual binding into a three-membered fragment of the infinite supramolecular chain (Fig. 3b). The additional structural stabilization of the discussed pseudopolymeric chain is achieved due to the paired secondary interactions Tl(2)···O(3)^a/O(4)^b and O(3)/O(4)···Tl(2)^b/ Tl(2)^a 3.259/3.290 Å (for comparison, the sum of the van der Waals radii of the interacting atoms is 3.46 Å [25, 26]). The following distinctions are characteristic of the pseudopolymeric chain formed by alternating molecules *A* including the Tl(1) and Tl(1)' atoms: (a) a greater diversity of the nonequivalent secondary Tl···S bonds (Table 2, Fig. 3a); and (b) only 50% oxygen atoms participate in secondary, but more significant, interactions Tl(1)/Tl(1)'^{b}···O(1)^a/O(1)' 3.04(2) Å; the distance from two other oxygen atoms O(2)' and O(2)^b to the nearest thallium atoms is already 4.469(12) and 4.554(11) Å, respectively. It should be mentioned that the combined manifestation of the secondary Tl···S and Tl···O interactions has previously been found also in the thallium(I) morpholinedithiocarbamate structure with the supramolecular self-assembly of its 3D pseudopolymeric framework [30].

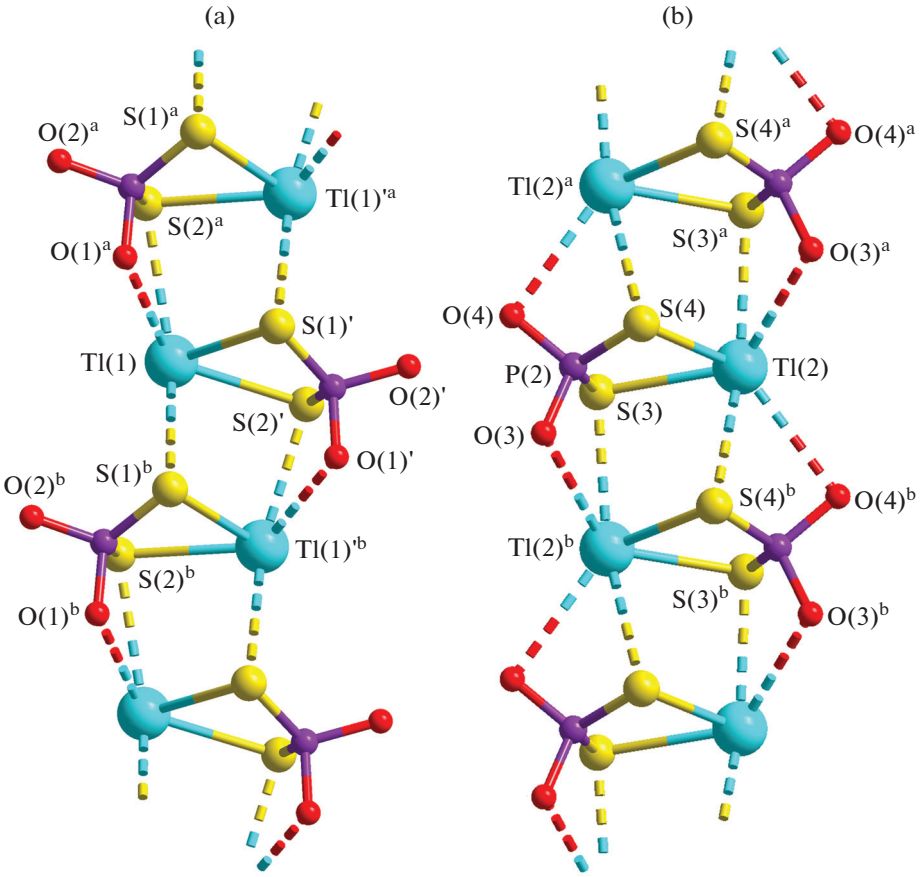

Fig. 3. Construction of the supramolecular pseudopolymeric chains by molecules (a) *A* and (b) *B*. Intermolecular secondary Tl···S and Tl···O interactions are shown by dashed lines. Symmetry transforms: [a] x, $3/2 - y$, $1/2+ z$; [b] x, $3/2 - y$, $-1/2 + z$. Alkyl substituents are omitted.

In addition, numerous paired secondary Tl···S interactions additionally occur between the pseudopolymeric chains of the $(\cdots A\cdots A\cdots A\cdots)_n$ and $(\cdots B\cdots B\cdots B\cdots)_n$ types resulting in the formation of a double supramolecular ribbon. The combinig mode of heterogeneous chains involving molecules *A*, which includethe Tl(1) and Tl(1)' atoms, is shown in Fig. 4. In the first case, molecules *A* and *B* from the neighboring chains form two nonequivalent secondary bonds: Tl(1)···S(3)[b] (3.335(2) Å) and Tl(2)[b]···S(2)' (3.338(3) Å). Two nonequivalent bonds are also formed in the second section: Tl(1)'[a]···S(3) 3.427(2) Å and Tl(2)···S(2)[a] 3.559(3) Å. Although these are the weakest secondary Tl···S interactions, their numerosity provides binding of two pseudopolymeric chains into the supramolecular ribbon. As compared to the published structures of thallium(I) dithiophosphates [7–10], a specific feature of the supramolecular chains formed by complex **I** is the complete unification of the character of binding between the neighboring molecular structural units.

The thermal behavior of compound **I** (transparent thin needles with an average size of 2.280 × 0.124 mm) in an argon atmosphere was studied by the STA method providing the parallel detection of TG and DSC curves (Fig. 5). The course of the TG curve indicates the thermal stability of the complex below ~170°C. The intense thermolysis of the substance formally occurs in one stage in a narrow temperature range of 170–270°C, where the TG curve has the main mass loss step equal to 39.41% (Fig. 5, *a*) with the maximum loss rate at 222.2°C. The subsequent slope region of the TG curve (270–465°C) is due to the smooth desorption of the thermolysis products (3.00%), after which the weight of the residual substance is stabilized (57.42%) and remains unchanged to the end of measurements at 700°C. It is important for an analysis of the TG data that the thermal dissociation of two alkoxy groups $-OC_5H_{11}$ of the Dtph ligand in complex **I** provides a mass loss of 36.79%. Therefore, somewhat higher experimental mass loss (42.41%) directly indicates that the inorganic moiety of the complex is also involved in the thermolysis.

The DSC curve shows a number of sequential endoeffects (Fig. 5, *b*). The most intense low-temperature endoeffect with the extreme at 76.4°C, which

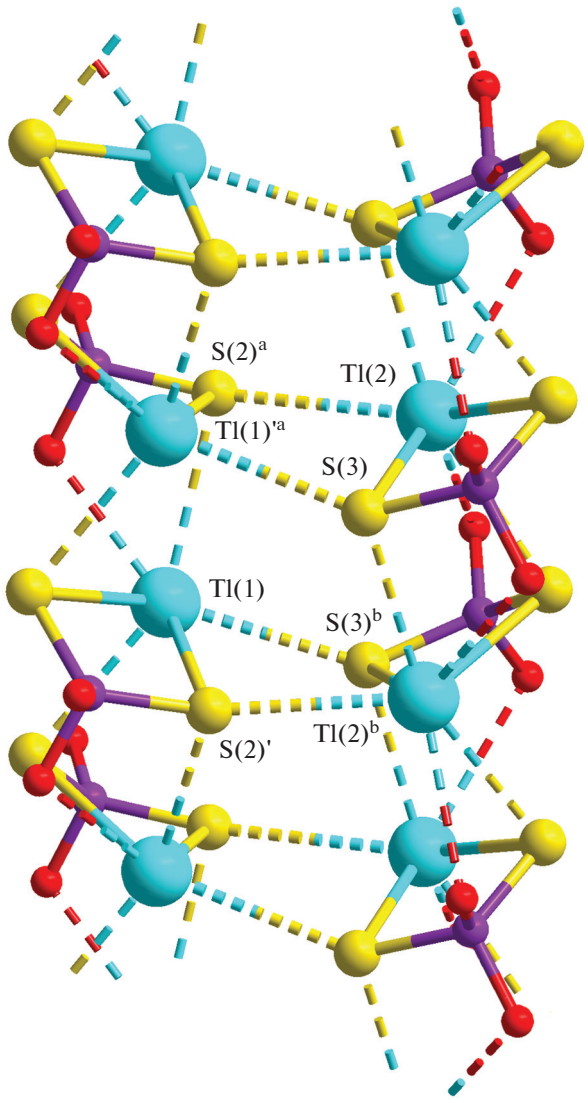

Fig. 4. Combination of the neighboring pseudopolymeric chains with the formation of the double supramolecular ribbon. All nonequivalent secondary interactions between the chains are presented. Symmetry transforms: [a] x, $3/2 - y$, $1/2 + z$; [b] x, $3/2 - y$, $-1/2 + z$.

is observed already before the mass loss onset, is caused by melting of the sample (the extrapolated m.p. 74.4°C). The melting was found in a range of 73–74°C by the independent determination (in a glass capillary). Three sequential endoeffects are low-intensity and weakly pronounced (with extremes at 220.7, 231.9, and 243.0°C) and are projected onto the steeply descending step of the TG curve associated with the main mass loss. This indicates a complicated character of the thermolysis consisting of a number of sequential thermal transformations of the substance.

When opening the crucible after cooling, a dark gray lustrous finely crystalline residue was observed on the bottom, which was then studied using SEM and EPMA. The enlarged plan of the crucible bottom with intergrown pieces of macroaggregates of the residual substance and its particle size, shape, and microstructure are shown in Figs. 6a and 6b. In spite of evident morphological and dimensional differences between particles of the studied substance (Fig. 6b), the use of the EPMA method did not allow us to reveal any variations in the chemical composition. The experimental energy dispersive spectra are nearly identical (Fig. 6c) and contain the characteristics peaks of thallium, sulfur, and phosphorus. (The presence of the aluminum peak is probably caused by the fact that the thermal behavior of compound **I** was studied in a corundum crucible.)

The data on studying the phase diagram of the binary $Tl_2S–P_4S_{10}$ system [31] (in which the formation of two thallium(I) thiophosphates, Tl_3PS_4 and $Tl_2P_2S_6$, was observed) seem to be important for the identification of the substance (containing only Tl, P, and S atoms) that was obtained during thermolysis of complex **I** under an argon atmosphere. The both compounds were also isolated in a preparative yield and structurally characterized [32, 33]. In addition, for Tl_3PS_4, which exhibits semiconducting properties [34], the experimental and theoretical studies (including quantum mechanical calculations [35]) of the electronic and electron-energy structures [36, 37] were performed.

The calculation of the residual weight of the substance during the thermolysis of complex **I** with the formation of thallium(I) tetrathiophosphate gives a value of 54.35%. The experimentally obtained value (57.42%) only slightly exceeds the calculated one. The mentioned weight exceeding can be due to the partial formation of elemental carbon, which is often observed for the thermal decomposition of substances bearing organic groups in an inert atmosphere.

In summary, the new thallium(I) di-*iso*-pentyl dithiophosphate, $[Tl\{S_2P(O\text{-}iso\text{-}C_5H_{11})_2\}]$, was isolated in a preparative yield and characterized in detail by XRD, STA, multinuclear (^1H, ^{13}C, ^{31}P) NMR, and IR spectroscopy. The complex in the crystalline state is presented by two (1 : 1) types of structurally nonequivalent molecules (*A* and *B*) in which the metal atom coordinates the single Dtph ligand iin an anisobidentate mode, forming the small-size four-membered metallocycle $[TlS_2P]$ in a 'butterfly' conformation. Each of the molecules constructs the pseudopolymeric chain of the $(\cdots A\cdots A\cdots A\cdots)_n$ or $(\cdots B\cdots B\cdots B\cdots)_n$ type due to the intermolecular paired secondary Tl···S and Tl···O bonds. In turn, numerous nonequivalent secondary Tl···S interactions (but weaker) also occur between these heterogeneous

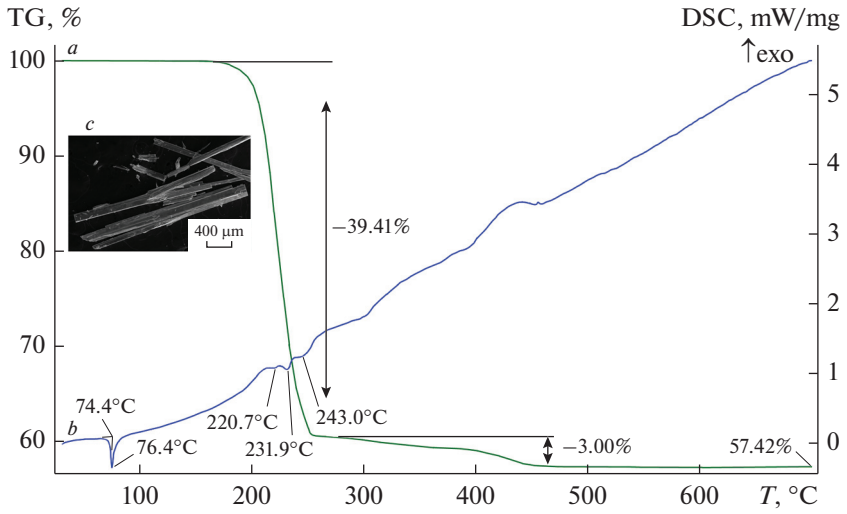

Fig. 5. (*a*) TG and (*b*) DSC curves and (*c*) the size and shape of the crystals of compound **I**.

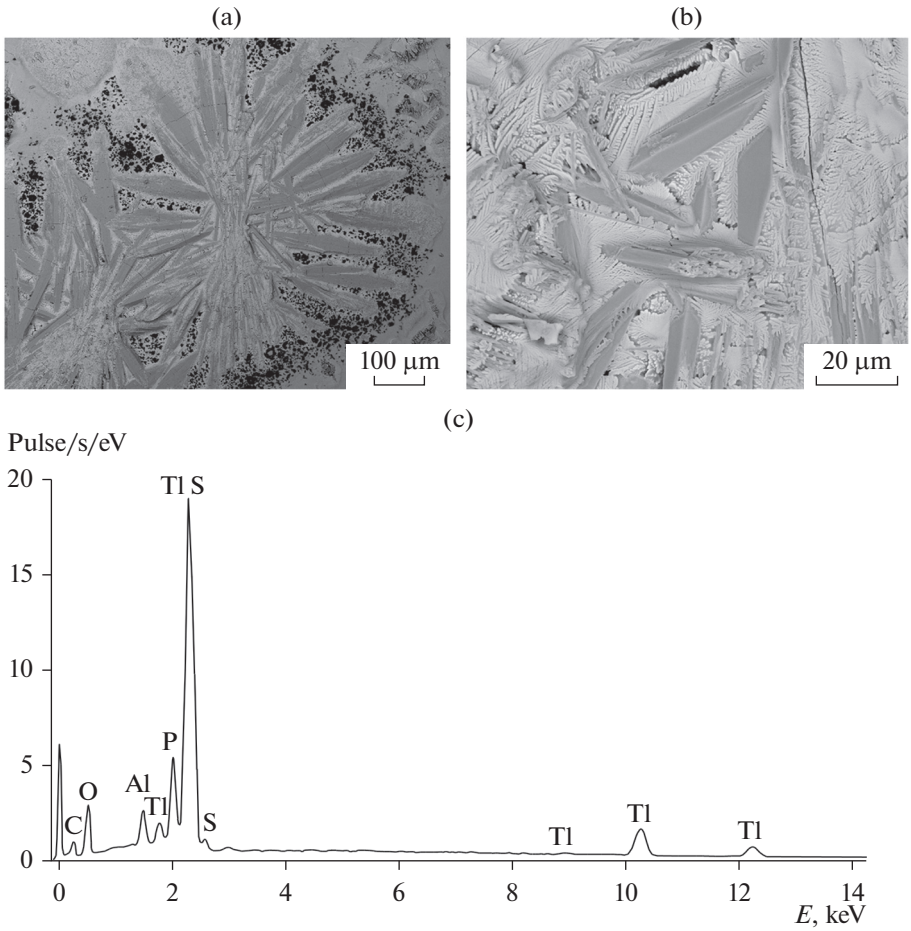

Fig. 6. (a) Enlarged fragment of the crucible bottom with the residual substance remaining after thermolysis of compound **I**; (b) the particle size, shape, and microstructure of the substance; and (c) its energy dispersive spectrum.

chains to form the double supramolecular ribbon. Thus, despite the relatively simple composition, the resulting thallium(I) di-iso-amyl dithiophosphate demonstrates the ability to self-organize a complicated supramolecular structure. The study of the thermal behavior of the complex showed that its thermolysis in an inert argon atmosphere occurred under rather mild conditions and in a narrow temperature range. According to the data of the EPMA and TG methods, thallium(I) tetrathiophosphate Tl_3PS_4 is the residual substance remained after thermolysis.

SUPPLEMENTARY INFORMATION

The online version contains supplementary material available at https://doi.org/10.1134/S1070328424600529.

ACKNOWLEDGMENTS

XRD data were obtained using the scientific equipment of the Center for Collective Use of Molecule Structure Investigation at the Nesmeyanov Institute of Organoelement Compounds (Russian Academy of Sciences) supported by the Ministry of Science and Higher Education of the Russian Federation (state assignment no. 075-03-2023-642). Elemental analysis and IR spectral studies were carried out on the equipment of the Center for Collective Use of Physical Methods of Investigation at the Kurnakov Institute of General and Inorganic Chemistry (Russian Academy of Sciences). Analytical studies of the residual substance were conducted at the Amur Center for Mineralogical and Geochemical Research of the Institute of Geology and Nature Management (Far Eastern Branch, Russian Academy of Sciences) (Laboratory of Microscopy and Structural and Molecular Research).

FUNDING

This work was supported by ongoing institutional funding. No additional grants to carry out or direct this particular research were obtained.

CONFLICT OF INTEREST

The authors of this work declare that they have no conflicts of interest.

REFERENCES

1. Sánchez-Chapul, L., Santamaría, A., Aschner, M., et al., *Front. Genet.*, 2023, vol. 14, p. 1168713.
2. Abdolmaleki, S., Ghadermazi, M., and Aliabadi, A., *Sci. Rep.*, 2021, vol. 11, p. 15699.
3. Sivagurunathan, G.S., Ramalingam, K., and Rizzoli, C., *Polyhedron*, 2013, vol. 65, p. 316.
4. Gomathi, G., Thirumaran, S., and Ciattini, S., *Polyhedron*, 2015, vol. 102, p. 424.
5. Manar, K.K., Rajput, G., Yadav, M.K., et al., *ChemistrySelect*, 2016, vol. 1, no. 18, p. 5733.
6. Liu, X.Z., Xue, H., Zhao, J., et al., *Rare Metals*, 1998, vol. 17, no. 3, p. 232.
7. Ivanov, A.V., Konfederatov, V.A., Gerasimenko, A.V., and Larsson, A.-C., *Russ. J. Coord. Chem.*, 2009, vol. 35, no. 11, p. 857. https://doi.org/10.1134/S1070328409110116
8. Rodina, T.A., Ivanov, A.V., Konfederatov, V.A., et al., *Russ. J. Inorg. Chem.*, 2009, vol. 54, no. 11, p. 1779. https://doi.org/10.1134/S0036023609110138
9. Firdoos, T., Kumar, P., Radha, A., et al., *New J. Chem.*, 2022, vol. 46, no. 2, p. 832.
10. Firdoos, T., Kumar, P., Sharma, N., et al., *CrystEngComm*, 2023, vol. 25, no. 26, p. 3777.
11. Sheldrick, G.M., *Acta Crystallogr., Sect. A: Found. Adv.*, 2008, vol. 64, no. 1, p. 112.
12. Sheldrick, G.M., *Acta Crystallogr., Sect. A: Found. Adv.*, 2015, vol. 71, no. 1, p. 3.
13. Dolomanov, O.V., Bourhis, L.J., Gildea, R.J., et al., *J. Appl. Crystallogr.*, 2009, vol. 42, no. 2, p. 339.
14. Kazitsyna, L.A. and Kupletskaya, N.B. *Primenenie UF-, IK-, YaMR- i mass-spektroskopii v organicheskoi khimii* (Application of UV, IR, NMR, and Mass Spectroscopy), Moscow: Mosk. Univ., 1979.
15. Rockett, J., *Appl. Spectrosc.*, 1962, vol. 16, no. 2, p. 39.
16. Mehrotra, R.C., Srivastava, G., and Chauhan, B.P.S., *Coord. Chem. Rev.*, 1984, vol. 55, no. 3, p. 207.
17. Bellamy, L.J., *The Infrared Spectra of Complex Molecules*, New York: Wiley, 1958.
18. Ahmad, R., Srivastava, G., and Mehrotra, R.C., *Inorg. Chim. Acta*, 1984, vol. 89, no. 1, p. 41.
19. Rodina, T.A., Korneeva, E.V., Antzutkin, O.N., and Ivanov, A.V., *Spectrochim. Acta, Part A*, 2015, vol. 149, p. 881.
20. Rodina, T.A., Ivanov, A.V., Gerasimenko, A.V., et al., *Polyhedron*, 2011, vol. 30, no. 13, p. 2210.
21. Larsson, A.-C., Ivanov, A.V., Antzutkin, O.N., and Forsling, W., *J. Colloid Interface Sci.*, 2008, vol. 327, no. 2, p. 370.
22. Ivanov, A.V., Antzutkin, O.N., Forsling, W., and Rodionova, N.A., *Russ. J. Coord. Chem.*, 2003, vol. 29, no. 5, p. 301. https://doi.org/10.1023/A:1023611415080
23. Ivanov, A.V., Larsson, A.-C., Rodionova, N.A., et al., *Russ. J. Inorg. Chem.*, 2004, vol. 49, no. 3, p. 373.
24. Alcock, N.W., *Adv. Inorg. Chem. Radiochem.*, 1972, vol. 15, no. 1, p. 1.
25. Bondi, A., *J. Phys. Chem.*, 1964, vol. 68, no. 3, p. 441.
26. Bondi, A., *J. Phys. Chem.*, 1966, vol. 70, no. 9, p. 3006.
27. Alvarez, S., *Dalton Trans.*, 2013, vol. 42, no. 24, p. 8617.
28. Hu, S.-Z., Zhou, Z.-H., and Robertson, B.E., *Z. Kristallogr.*, 2009, vol. 224, no. 8, p. 375.
29. Allinger, N.L., Zhou, X., and Bergsma, J., *J. Mol. Struct.: THEOCHEM.*, 1994, vol. 312, no. 1, p. 69.

30. Bredyuk, O.A., Loseva, O.V., Ivanov, A.V., et al., *Russ. J. Coord. Chem*., 2017, vol. 43, no. 10, p. 638. https://doi.org/10.1134/S1070328417100013

31. Andrae, H. and Blachnik, R., *J. Alloys Compd.*, 1992, vol. 189, no. 2, p. 209.

32. Toffoli, P., Khodadad, P., and Rodier, N., *Bull. Soc. Chim. Fr.*, 1981, nos. 11/12, p. 429.

33. Wibbelmann, C., Brockner, W., Eisenmann, B., and Schäfer, H., *Z. Naturforsch., B: Chem. Sci.,* 1983, vol. 38, no. 12, p. 1575.

34. Lavrentyev, A.A., Gabrelian, B.V., Nikiforov, I.Ya., et al., *Phys. Scr.*, 2005, vol. T115, p. 162.

35. Lavrentyev, A.A., Gabrelian, B.V., Vu, V.T., et al., *Bull. Russ. Acad. Sci. Phys*., 2015, vol. 79, no. 6, p. 802. https://doi.org/10.3103/S1062873815060179

36. Lavrentyev, A.A., Gabrelian, B.V., Nikiforov, I.Ya., et al., *J. Phys. Chem. Solids*, 2003, vol. 64, no. 12, p. 2479.

37. Lavrentyev, A.A., Gabrelian, B.V., Vu, V.T., et al., *J. Struct. Chem*., vol. 58, no. 6, p. 1220. https://doi.org/10.1134/S002247661706021X

Translated by E. Yablonskaya